Supporting information for "Determination of radiative and multiphonon non-radiative relaxation rates of upconversion materials

Lin Fu[1], Yusong Wu[1], Changxian Zhang[2], Tairan Fu[1,*], Congling Shi[3,**]

1. Key Laboratory for Thermal Science and Power Engineering of Ministry of Education, Beijing Key Laboratory of CO_2 Utilization and Reduction Technology, Department of Energy and Power Engineering, Tsinghua University, Beijing 100084, P. R. China
2. Aero Engine Academy of China, Beijing 101304, P. R. China
3. China Academy of Safety Science & Technology, Beijing 100029, P.R. China

Corresponding Author

E-mail: *, trfu@mail.tsinghua.edu.cn; **, 29143953@qq.com

1. X-ray diffraction

Figure S1 illustrates the XRD patterns of the synthesized powders. It can be observed from the XRD patterns that all the peaks can be indexed to the β-$NaYF_4$ phase, conforming to JCPDS standard card No. 16-0334. The crystal unit cell parameters are calculated to be (a=5.978 Å, c=3.525Å) for sample #A, (a=5.945Å, c=3.495Å) for sample #B, and (a=5.957Å, c=3.505Å) for sample #C using the XRD data. Overall, the calculated parameters are consistent with the standard values (a=5.96Å, c=3.53Å) on JCPDS card No. 16-0334. No other impurity phases were observed in Fig. S1, suggesting that the doped Er^{3+} ions were successfully inserted into the host lattices and have no influence on the crystal structures. Miller indices are also marked in the figure.

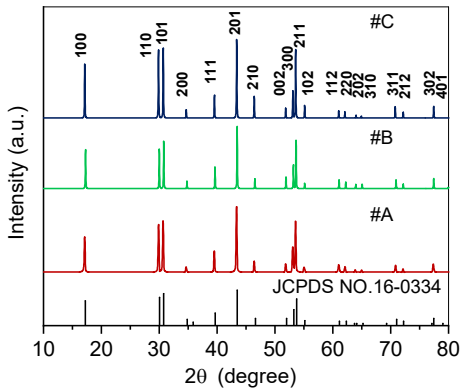

Fig. S1 XRD patterns of the samples and the standard pattern of β-$NaYF_4$ (JCPDS NO.16-0334) is displayed as a reference

2. SEM

Figure S2 exhibits the SEM micrographs of the synthesized powders. The powder samples formed a microcrystalline structure with grain size mainly distributed in 1~2 μm. All the samples are composed of irregular grains with a rough surface and less aggregation.

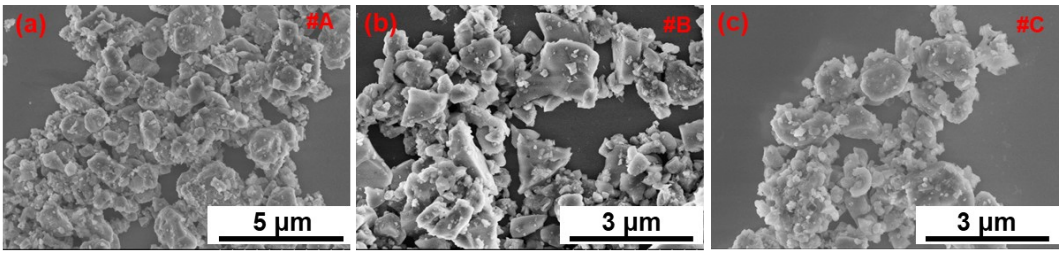

Fig. S2 SEM images of samples (a) #A, (b) #B, and (c) #C.

3. Selection of the excitation power density

The most possible energy transfer upconversion mechanisms for Er^{3+} are:

$$^4I_{13/2}+^4I_{13/2}\rightarrow ^4I_{9/2}+^4I_{15/2},\ ^4I_{9/2}\rightarrow ^4I_{11/2}+nh\omega \quad (1)$$

$$^4I_{11/2}+^4I_{11/2}\rightarrow ^4F_{7/2}+^4I_{15/2},\ ^4F_{7/2}\rightarrow ^2H_{9/2}\ (^4S_{3/2})+nh\omega \quad (2)$$

Where $h\omega$ represents the maximum phonon energy of the matrix lattice, $h\omega$ is about 450cm^{-1} [1] for β-$NaYF_4$; n represents the number of phonons released in the multiphonon relaxation process, usually n<5. In mechanism (1), the ions upconversion to $^4I_{9/2}$ level will rapidly relax to $^4I_{11/2}$ level through the multiphonon relaxation process. In mechanism (2), two ions at $^4I_{11/2}$ level undergo energy transfer upconversion, so that one of them transitions to $^4F_{7/2}$ level and relax to $^2H_{9/2}(^4S_{3/2})$ level rapidly. $^4I_{9/2}$ level and $^4I_{11/2}$ level as main participating energy levels in upconversion processes, the luminescence from which level will show a nonlinear law to the excitation power density when upcoversion happened. Therefore, we can judge whether the energy transfer upconversion processes need to be considered by measuring the excitation power density dependence of the luminescence intensity of the two energy levels. If the luminous intensity changes linearly with excitation power density, it indicates that the energy transfer upconversion phenomenon in the process can be ignored. If it is nonlinear, it indicates that the energy transfer upconversion is very important in the process. Furthermore, we can determine the excitation power selection range based on this experiment.

In Fig. S3, the ranges in which the luminescence emission intensities of the upconversion energy levels vary linearly with the excitation power densities are shown for all the sub-systems. In the measurements, the power densities used are 0.03 W/cm^2 for the three-level system, 0.8 W/cm^2 for the four-level system, 0.15 W/cm^2 for the five-level system, and 0.06 W/cm^2 for the six-level system.

For the two-level system, the power density used is 0.02 W/cm^2, and no upconversion luminescence was observed in the emission spectrum[2].

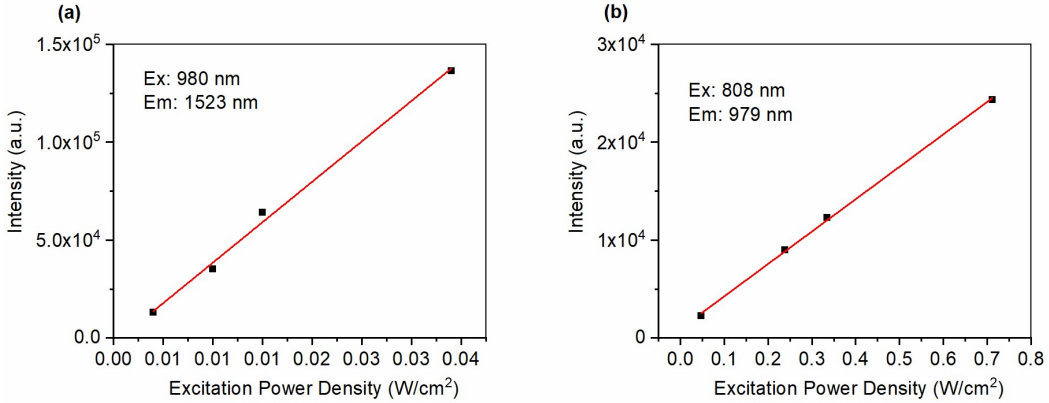

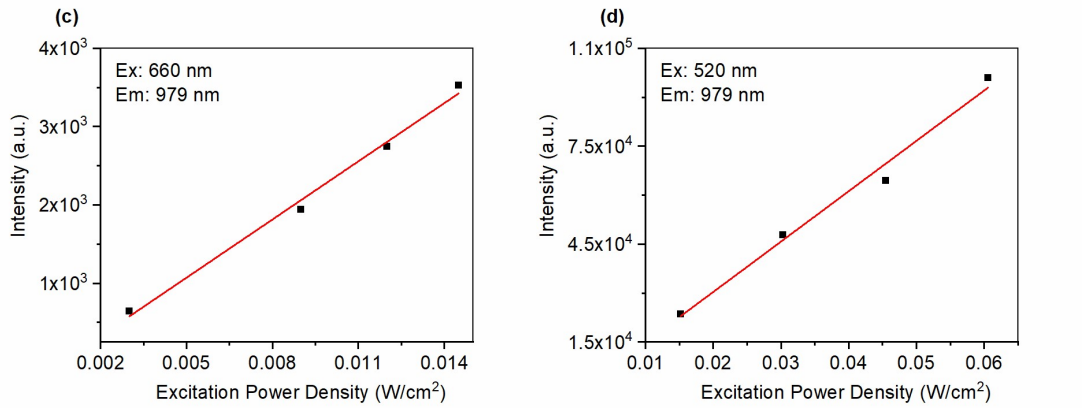

Fig. S3 Power density dependence of the luminescence intensity for (a) Three-level system, (b) Four-level system, (c) Five-level system and (d) Six-level system.

4. Calculation of the intensity ratio

In Fig. S4, we show the normalized spectrum of the emitted photons in different systems. The color filling part is the area for integration. The integral values obtained and the intensity ratios required in the calculation are given in Table S1.

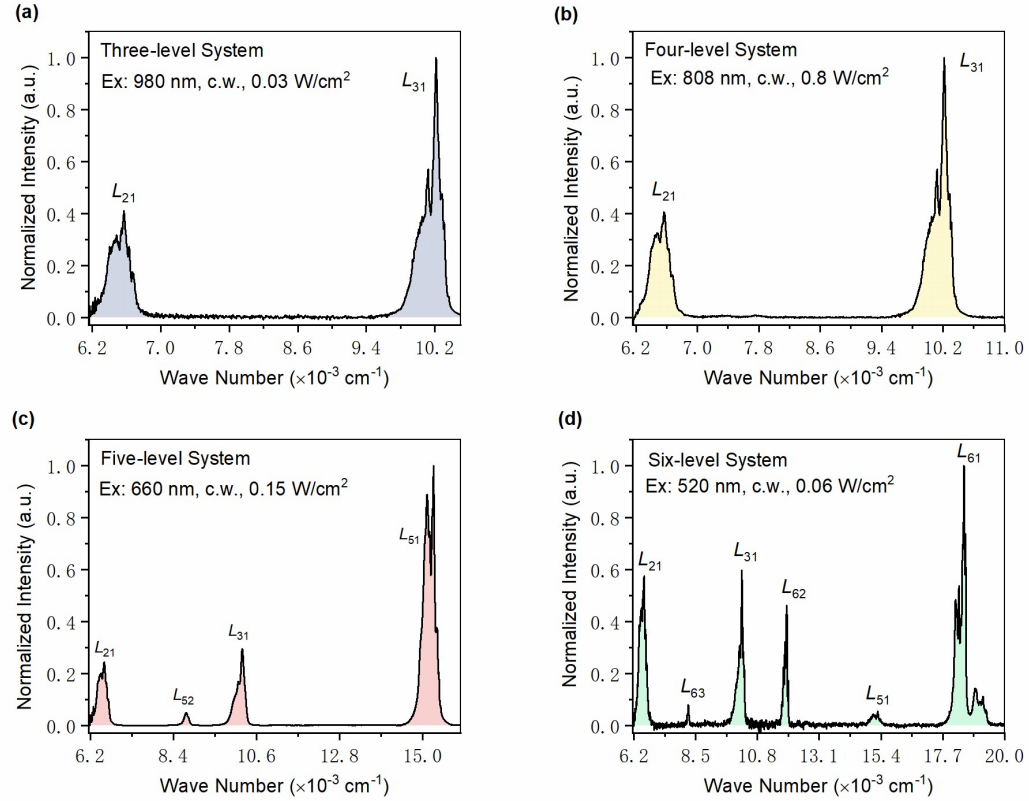

Fig. S4 Integral areas (filled with color) of emission peaks for (a) Three-level system, (b) Four-level system, (c) Five-level system and (d) Six-level system.

Table S1 Integration results and intensity ratios of the multi-level systems

System	Integrated result /a.u.	Intensity ratio
Three-level	$L_{21} = 106.8$ $L_{31} = 203.5$	$L_{31} / L_{21} = 1.90$
Four-level	$L_{21} = 108.1$ $L_{31} = 203.3$	$L_{31} / L_{21} = 1.88$
Five-level	$L_{21} = 68.0$ $L_{52} = 7.9$ $L_{31} = 69.6$ $L_{51} = 333.9$	$L_{51} / L_{31} = 4.80$ $L_{31} / L_{52} = 8.81$ $L_{31} / L_{21} = 1.02$
Six-level	$L_{21} = 140.9$ $L_{63} = 6.2$ $L_{31} = 114.8$ $L_{62} = 63.5$ $L_{51} = 19.8$ $L_{61} = 318.8$	$L_{61} / L_{51} = 16.12$ $L_{51} / L_{62} = 0.31$ $L_{21} / L_{63} = 22.72$ $L_{31} / L_{63} = 18.47$ $L_{31} / L_{62} = 1.81$

Reference

1. A. Teitelboim, B. Tian, D. J. Garfield, A. Fernandez-Bravo, A. C. Gotlin, P. J. Schuck, B. E. Cohen and E. M. Chan, *The Journal of Physical Chemistry C*, 2019, **123**, 2678-2689.
2. L. Fu, Y. Wu and T. Fu, *Journal of Luminescence*, 2022, **245**, 118758.